Photolithography-free polymer optical waveguide arrays for optical backplane bus

Xinyuan Dou,[1] Alan X. Wang,[2] Xiaohui Lin,[1] and Ray T. Chen[1,2,*]

[1]*Department of Electrical and Computer Engineering, the University of Texas at Austin, Austin, TX 78758, USA*
[2]*Omega Optics, Inc., Austin, TX 78759, USA*
**chen@ece.utexas.edu*

Abstract: In this paper, an innovative 3-to-3 bi-directional optical bus architecture based on multimode polymer waveguides with embedded 45° micro-mirrors was successfully demonstrated. With a lithography-free imprinting process by high quality electroplated metallic mold, the device can be precisely replicated with a low fabrication cost. Superior to any point-to-point optical waveguide, the implemented optical bus structure is capable of broadcasting and receiving high speed data at 10Gbit/sec among multiple points as a high performance optical backplane.

OCIS codes: (200.4650) Optical interconnects; (130.5460) Polymer waveguides; (230.0230) Optical devices.

References and links

1. D. Huang, T. Sze, A. Landin, R. Lytel, and H. L. Davidson, "Optical interconnects: out of the box forever?" IEEE J. Sel. Top. Quantum Electron. **9**(2), 614–623 (2003).
2. R. T. Chen, L. Lin, C. Choi, Y. J. Liu, B. Bihari, L. Wu, S. Tang, R. Wickman, B. Picor, M. K. Hibbs-Brenner, J. Bristow, and Y. S. Liu, "Fully embedded board-level guided wave optoelectronic interconnects," Proc. IEEE **88**(6), 780–793 (2000).
3. A. L. Glebov, M. G. Lee, and K. Yokouchi, "Integration technologies for pluggable backplane optical interconnect systems," Opt. Eng. **46**(1), 015403 (2007).
4. A. Flores, S. Song, J. J. Yang, Z. Q. Liu, and M. R. Wang, "High-speed optical interconnect coupler based on soft lithography ribbons," J. Lightwave Technol. **26**(13), 1956–1963 (2008).
5. K. Gicherl, X. Han, and R. T. Chen, "A method for rebroadcasting signals in an optical backplane bus system," J. Lightwave Technol. **19**, 959–965 (2002).
6. X. Han, G. Kim, G. J. Lipovski, and R. T. Chen, "An optical centralized shared-bus architecture demonstrator for microprocessor-to-memory interconnects," IEEE J. Sel. Top. Quantum Electron. **9**(2), 512–517 (2003).
7. X. Han, G. Kim, and R. T. Chen, "Accurate diffraction efficiency control for multiplexed volume holographic gratings," Opt. Eng. **41**(11), 2799–2802 (2002).
8. H. Bi, X. Han, X. Chen, W. Jiang, J. Choi, and R. T. Chen, "15Gbps bit-interleaved optical backplane bus using volume photo-polymer holograms," IEEE Photon. Technol. Lett. **18**(20), 2165–2167 (2006).
9. M. Tan, P. Rosenberg, J. S. Yeo, M. McLaren, S. Mathai, T. Morris, J. Straznicky, N. P. Jouppi, H. P. Kuo, S. Wang, S. Lerner, P. Kornilovich, N. Meyer, R. Bicknell, C. Otis, and L. Seals, "A high-speed optical multi-drop bus for computer interconnections," in 16th IEEE Symposium on High Performance Interconnects (2008).
10. X. Y. Dou, X. Wang, H. Y. Huang, X. H. Lin, D. Ding, D. Z. Pan, and R. T. Chen, "Polymeric waveguides with embedded micro-mirrors formed by Metallic Hard Mold," Opt. Express **18**(1), 378–385 (2010).
11. D. Xinyuan, X. Wang, X. H. Lin, D. Ding, D. Z. Pan, and R. T. Chen, "Highly flexible polymeric optical waveguide for out-of-plane optical interconnects," Opt. Express **18**(15), 16227–16233 (2010).
12. X. Wang, W. Jiang, L. Wang, H. Bi, and R. T. Chen, "Fully embedded board level optical interconnects-from waveguide fabrication to device integration," J. Lightwave Technol. **26**(2), 243–250 (2008).

1. Introduction

Conventional optical interconnect using point-to-point optical waveguide or waveguide array fails to provide non-congestional interconnection among multiple points, which is due to the intrinsic nature of such architectural topology [1–4]. Such a point-to-point optical interconnect structure is useful to most high performance computer (HPC) system only when it is combined with electrical switch backplanes. This topological deficit critically restricts the gain in the bandwidth capacity, because it cannot carry out multicast/broadcast as effectively as the backplane bus can do [5]. For such hybrid optical-electrical system, besides the hop delay, each data transfer phase inevitably incurs a routing overhead, which makes it rather

#147768 - $15.00 USD Received 18 May 2011; revised 28 Jun 2011; accepted 1 Jul 2011; published 12 Jul 2011

difficult to minimize the overall interconnect latency. In order to overcome these challenges, we have demonstrated an optical backplane bus that are based on substrate-guided optical interconnects [5–8], which is a direct network to possess very high connectivity. For example, optical centralized shared bus architecture in uniprocessing systems has been experimentally verified by applying it to fulfill the critical microprocessor-to-memory interconnects [6]. However, such substrate-guided optical bus structures have intrinsic drawbacks in packaging density and stability concerns comparing with optical waveguide approaches [8]. A master-slave parallel optical bus was reported based on pellicle beam splitters, but the fabrication processes are not cost-effective [9]. Here we designed a polymer waveguide based bi-directional optical bus system with 3-to-3 nodes, which have demonstrated the advantages of enhanced bandwidth, increased reliability, package compatibility and significantly lower fabrication cost.

2. Design of optical bus architecture

A planar view of the 3-to-3 optical bus architecture is shown in Fig. 1(a). It consists of two parallel optical bus waveguides, which can transmit optical signals along two opposite directions. The optical signals from the transmitter (T) of each transceiver will be split into two beams and transmitted bi-directionally into the two bus waveguides through two unidirectional branch waveguides. The receiver (R) of each transceiver is also capable of receiving optical signals from both of the two bus waveguides, benefited from the two unidirectional branch waveguides that are connected with them. The two parallel optical bus waveguides in conjunction with the unidirectional branch waveguides ensure completely non-blocking interconnection among any existing transceiver without any wiring crossing. The transmitter and receiver are located either on the associated cardboards or the optical backplane itself. The intra-plane interconnection, i.e., from the transmitters and receivers to the optical waveguides, are established through surface normal micro-mirrors. A simple implementation would be coupling optical waves into and out of the waveguide by a 45°micro-mirror and then split by a Y-branch splitter, as shown in Fig. 1(b).

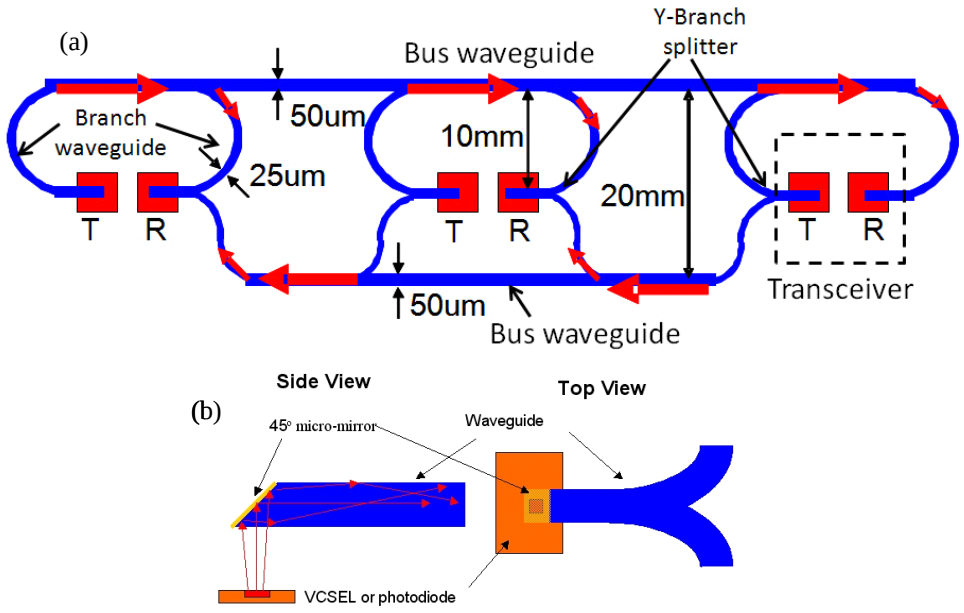

Fig. 1. (a) Schematic view of the 3-to-3 optical bus architecture (b) Intra-plane surface normal interconnection using 45°micro-mirror.

In this paper, we will not discuss detailed implementation of optical bus systems integrated with laser diodes, photodetectors, optoelectronic drivers and printed circuit boards.

#147768 - $15.00 USD Received 18 May 2011; revised 28 Jun 2011; accepted 1 Jul 2011; published 12 Jul 2011

Instead, we will highly focus on simple but pivotal topics: the feasibility of using polymer waveguides for optical bus architecture with the capability of broadcasting optical signals among multiple points. Using the same polymer waveguides as those in [10,11], the thickness of the polymer layer is fixed at 50μm. The width of the bus waveguides and the waveguide sections for micro-mirrors is 50 μm as well. But we do need some optical simulation to determine the other parameters of the optical bus architecture for best performance.

(1) Radius of the bending waveguide

The radius of the bending waveguide (branch waveguides in Fig. 1(a)) determined the waveguide loss as well as the size of the layout. Smaller radius could save more space, however, causing more radiation loss. Compared with single mode waveguides, whose bending loss can be easily simulated, multimode waveguides are much more complex since higher order modes can radiate much more quickly than the fundamental mode. Additionally, these higher order modes are mixed with each other, making the theoretical analysis based on guided wave optics extremely difficult. To simulate the bending loss of the multimode waveguides, we use a ray tracing method to simplify the design optimization. The light source we used for our simulation is an 850nm vertical cavity surface emitting laser (VCSEL) with half divergent angle of 5° and an aperture size of 10μm. The refractive indices of the cladding and core layer are 1.45 and 1.47, respectively. The input waveguide has a length of 1mm to stabilize the coupling condition. The curving waveguide, which has the same cross section as the input waveguide, bends 180 degree with a radius of R. Figure 2 shows the throughput optical power (defined as the output power / input power) as a function of the bending radius R for waveguide cross section of 50μm × 50μm (width × height) and 25μm × 50μm. The simulation results show that narrower waveguide can tolerate smaller bending radius. For the optical waveguide with 25μm × 50μm cross section, the largest throughput of 89% is reached when the bending radius is 5mm. Larger bending radius can cause higher optical loss due to longer waveguide length.

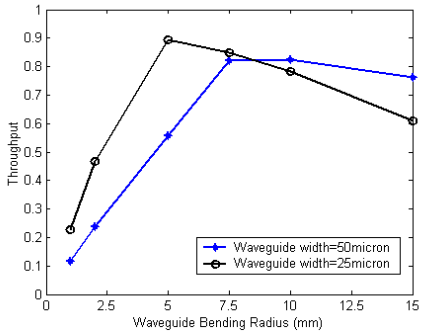

Fig. 2. Throughput optical power for waveguides with different radius.

(2) Coupling between the branch waveguide and the bus waveguide

Depending on how many transceivers are connected with the bus structure, the coupling ratio between the branch waveguides and the bus waveguides need to be adjusted for equal power distribution. Figure 3(a) shows the design of the connection between the bus waveguide and branch waveguide. The width of the branch waveguide is 25μm, and the bus waveguide is 50μm. The radius of the branch waveguide is R = 5mm, and the starting angle of this arc is zero degree. To achieve a large range of power splitting ratio, we dynamically tune the bus waveguide width W to a smaller value, but then gradually taper the width back to 50μm. In this fashion, various ratio of power can be coupled into the branch waveguides. The simulation result is shown in Fig. 3(b). As the width of the bus waveguide shrinks from 50μm to 25μm, the coupling efficiency can be dynamically tuned from 22% to 48%. This will provide sufficient design flexibility for the optical bus structure shown in Fig. 1, which

#147768 - $15.00 USD Received 18 May 2011; revised 28 Jun 2011; accepted 1 Jul 2011; published 12 Jul 2011

requires 33.3%, 50% and 100% power splitting ratio for the waveguide couplers connected to the upper bus waveguide, and 50% and 100% power splitting ratio for the waveguide couplers connected to the lower bus waveguide.

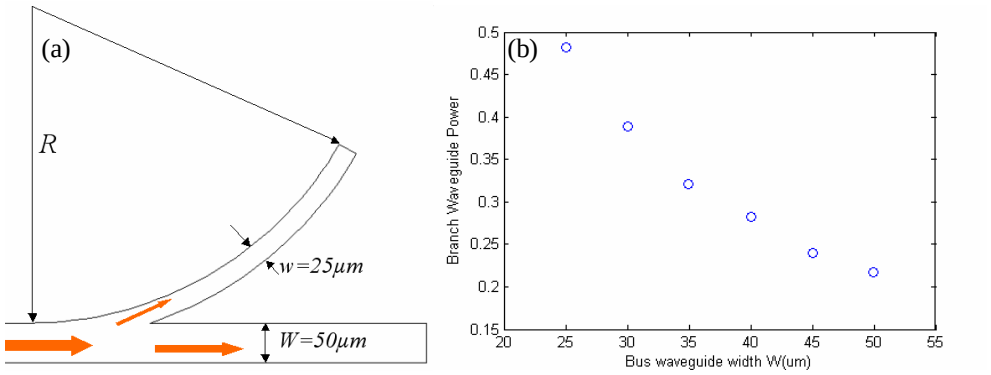

Fig. 3. (a) Schematics of the optical bus connection, (b) Coupling ratio as a function of the bus width W.

(3) Power splitting ratio between the two branch waveguides

In order to control the power splitting ratio of the Y-branch waveguide as shown in Fig. 1, we simply assume the optical power is evenly distributed across the multimode waveguide. Hence, by controlling the width ratio of the two splitting waveguide, one can obtain a proportional power balance. For example, if we want to evenly split the optical power, we can set both of the two branch waveguides to be 25μm; if the power splitting ratio is 25%: 75%, the width of the two waveguides is 12.5μm and 37.5μm respectively. Figure 4 is the ray tracing simulation result, which agrees very well with our simple assumption.

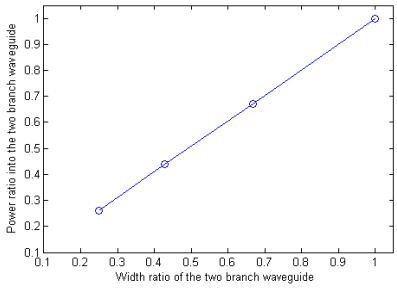

Fig. 4. Power splitting ratio as a function of the width of the two branch waveguides.

3. Preparation of optical bus pre-mold and metal Ni mold

The fabrication process for the bidirectional bus structure is completely compatible with parallel point-to-point optical interconnects waveguide that we have reported [10]. First, a photopolymer SU-8 based bus pre-mold with 45° surfaces was fabricated by tilted exposure under DI-water; then a certain thickness of Ni was electroplated into the SU-8 defined trenches. After the electroplating process, the SU-8 layer was removed and a metallic bus mold was achieved. Using the metallic bus mold, a polymeric optical bus device was formed by UV imprinting method using UV curable polymer WIR-30 series.

The schematic process to prepare the optical bus pre-mold is shown in Fig. 5. A layer of 50μm thick SU-8(from MicroChem) was first spin-coated onto a Ti/Au seed layer coated silicon substrate. Three exposures were carried out in order to achieve the bus waveguide pattern as well as the opposite-placed 45° surfaces. The first exposure was carried out through

#147768 - $15.00 USD Received 18 May 2011; revised 28 Jun 2011; accepted 1 Jul 2011; published 12 Jul 2011

vertical exposure to create the bus structure using the optical bus mask. The second and third exposures were carried out tilted under DI-Water to achieve 45° surfaces at the input and output node ends of the bus structure. The exposure setup under DI-water and the titled angle was calculated and described in detail else-where [10]. After the three exposures, post-exposure bake and developing were carried out to achieve a SU-8 based optical bus waveguide pre-mold.

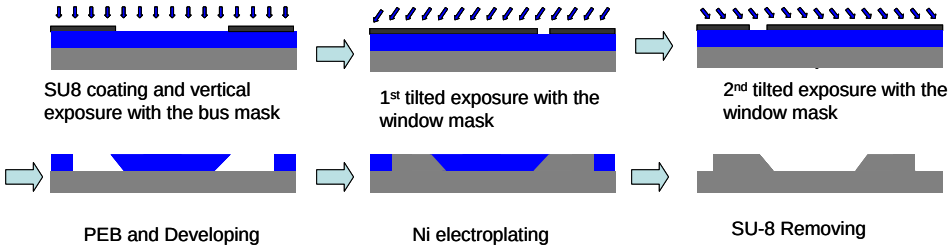

Fig. 5. Schematic view of the optical bus pre-mold and Ni mold fabrication with 45° tilted surfaces.

After successfully achieving the SU-8 based optical bus waveguide pre-mold, Ni metal was electroplated into the SU-8 defined bus structure trenches. Ni metal was grown on the seed layer where SU-8 was not covered. The detailed plating parameters were described in [10]. Normal plating current density is around 10mA/cm^2. To obtain a 50μm thickness of plated metal, total plating time is around 6-7hours. Small current density (<2mA/cm^2) was used at the beginning and the end of electroplating to achieve stronger adhesion and a smoother surface. After successfully plating Ni metal, the SU-8 pre-mold layer was removed by remover PG. The SU-8 residue was removed by O_2 plasma ashing.

The developed SU-8 based bus waveguide pre-mold was observed under scanning electron spectroscopy (SEM), shown in Fig. 6. Figure 6(a) shows one of the input nodes with a Y-branch coupler, inset image is a larger view of the pre-mold 45° coupling surface. Figure 6(b) shows the input and output nodes of the plated Ni hard mold with two opposite 45 surfaces. Inset image is the larger view of the 45° coupling surface of the Ni metal mold. The actual slant angle of the coupling surface was measured to be 45.5°, having a 0.5° deviation from the designed angle. We carried out a series of tilted exposure under DI-water and the slant angles for 10 samples were measured (Fig. 6(c)). The average angle is 45.3° with a standard deviation of 0.15°. This proves the slant angle can be controlled very well by tilted exposure under DI-water. By doing a series of electroplating process, 45° surface slant angles of 10 samples were also measured, as listed in Fig. 6(d). The average angle is 44.8° with a standard deviation of 0.27°. This is consistent very well with the SU-8 pre-mold slant angle measurement results.

#147768 - $15.00 USD Received 18 May 2011; revised 28 Jun 2011; accepted 1 Jul 2011; published 12 Jul 2011

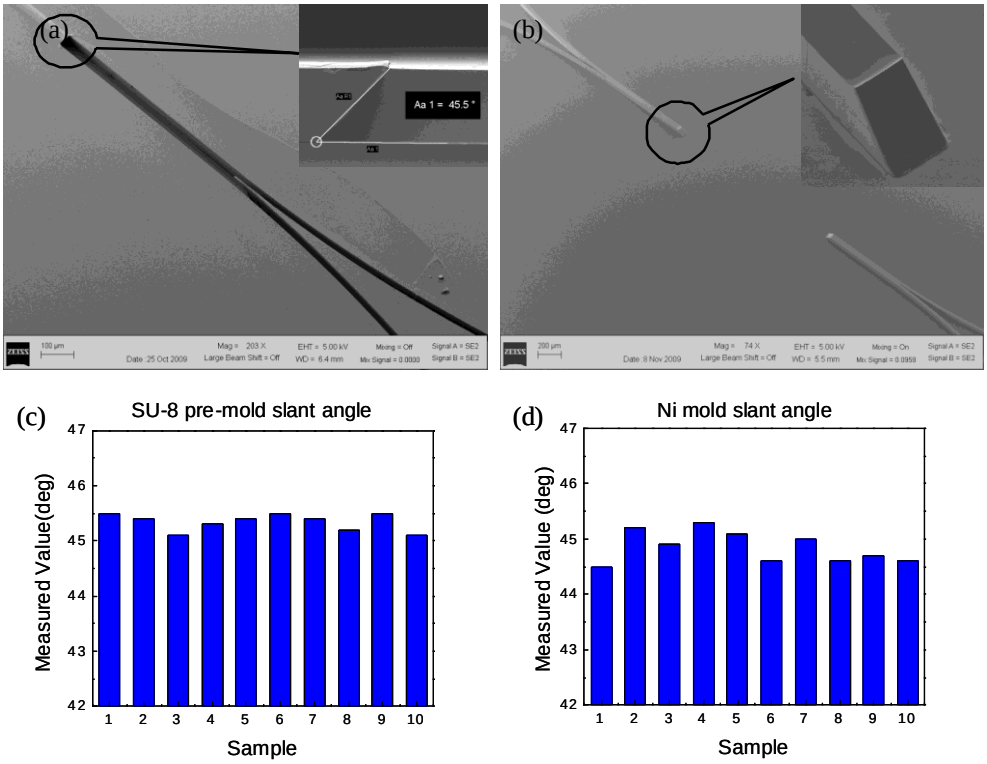

Fig. 6. SEM image of (a)SU-8 pre-mold of Y-branch splitter/coupler, (b) metal Ni mold. (c) Statistics of SU-8 pre-mold slant angle and (d) Statistics of metal Ni mold slant angle.

4. Imprint of polymeric optical bus waveguide

A polymeric optical bus waveguide was successfully fabricated using the electroplated Ni metal bus waveguide mold through a UV imprint method. UV curable polymers WIR30 series (from ChemOptics), WIR30-450 (n = 1.45@850nm), WIR30-470 (n = 1.47@850nm) were used for the waveguide cladding and core, respectively [12]. A 200μm thick TEONEX thin film (from Dupont Teijin Films Inc.) was used as the TOPAS substrate. The imprint process is shown in Fig. 7. Firstly, a thin bottom cladding layer of WIR-30-450 was coated on the TOPAS film followed by UV cure. A thin layer of AZ5209 photoresist was coated on the Ni bus hard mold as the release layer. Then, put the Ni bus hard mold onto the TOPAS film with WIR30-450 between the metal hard mold and the substrate, UV cure in N_2 atmosphere for 12min to solidify the polymer. Release the hard mold in acetone. In this way, the optical bus waveguide pattern was successfully transferred onto the WIR/substrate film. After detached from the Ni mold, 200nm of Au mirrors were coated at the input nodes and output nodes. Core material and top cladding were filled and coated followed by a UV cure process.

The imprinted optical bus waveguide were studied under SEM. Images were taken before the core filling process, shown in Fig. 8. Figure 8(a) shows an input node, which has a 1:2 power splitting ratio Y-branch splitter and a 45° surface-normal coupling mirror. Figure 8(b) is the SEM of the bus-branch coupler/splitter.

#147768 - $15.00 USD Received 18 May 2011; revised 28 Jun 2011; accepted 1 Jul 2011; published 12 Jul 2011

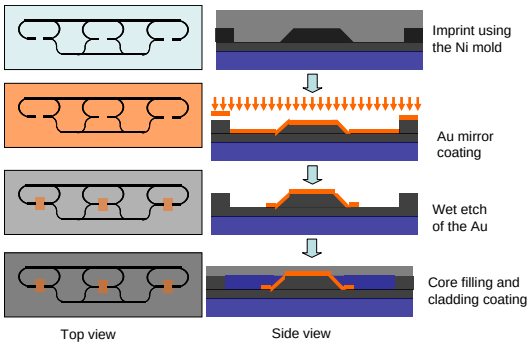

Fig. 7. UV imprint process to fabricate the polymeric optical bus waveguide using the Ni metal hard mold.

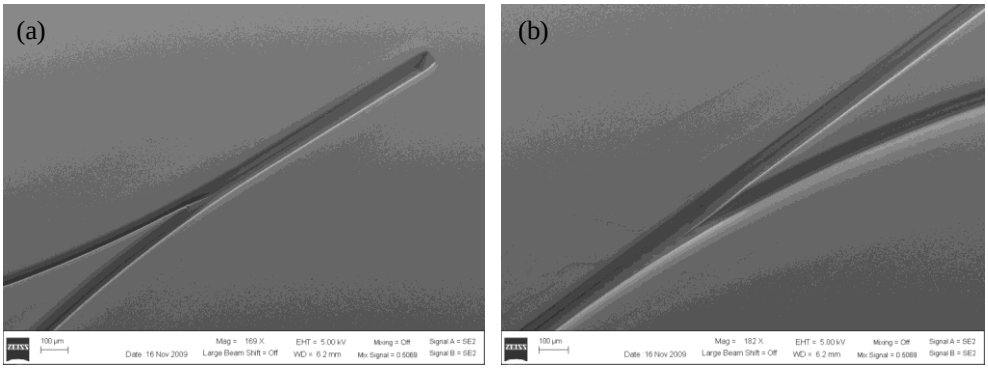

Fig. 8. SEM images of the optical bus waveguide after UV imprint. (a) Input node, Y splitter and 45° micro-mirror (b) Junction of the branch with the bus.

5. Testing on the polymeric bus waveguide

High speed testing on the fabricated optical bus waveguide was measured at 850nm wavelength. Before the testing, we used a red laser at 635nm to observe the output of the optical bus waveguide through microscope (Fig. 9(a)). A single mode fiber was fixed above the 45° micro-mirror region of the input node. Inset image in Fig. 9(a) is the optical output pattern on the monitor through microscope. After confirming the optical bus waveguide is working, we switched to 850nm wavelength to measure the output signal. An 850nm laser diode with a 9/125μm SMF pigtail was normally coupled into the bus waveguide input node through the 45° micro-mirror. The output power at the output nodes was measured by a photodetector, which was fixed just above the bus waveguide output nodes. The minimum insertion loss we can achieve is around 15dB. Comparing to the straight waveguide, this is higher due to the curved structure of the bus waveguide and the power splitting. High speed testing at 1Gbps and 10Gbps were carried out at 850nm. VCSELs and photodiodes (PD) operating at 850nm were purchased from Finisar Co.. The experimental setup of the high speed optical test is shown in Fig. 9(b), which has a signal generator, evaluation boards for VCSEL and photodiode connections, device stage, DC power supply and oscilloscope for eye-diagrams. A 50/125μm multi-mode fiber was used to couple the light from the VCSELs to the waveguide. In order to increase the coupling efficiency, a drop of water was used as an index-matching medium between the MMF and bus waveguide nodes. The testing operation details were described in reference [12].

#147768 - $15.00 USD Received 18 May 2011; revised 28 Jun 2011; accepted 1 Jul 2011; published 12 Jul 2011

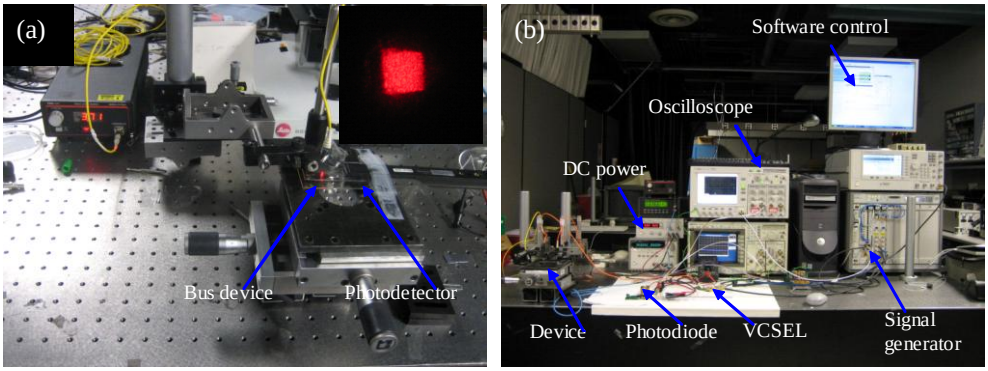

Fig. 9. (a) Insertion loss measurement and (b) High speed measurement setup for the bus waveguide.

We successfully obtained the eye-diagrams for the optical bus waveguide from 1Gbps to 10Gbps, shown in Fig. 10. The Q-factors of the eye-diagrams are measured with values from 6.23 to 4.67, respectively. The corresponding Bit-Error-Rates(BER) were calculated to be 2.3×10^{-10} and 1.5×10^{-6} for 1Gbps and 10Gbps, respectively if assuming the Gaussian distributed noises [12]. Further research work is on-going to reduce the insertion loss and increase the Q-factors for the optical bus waveguide device.

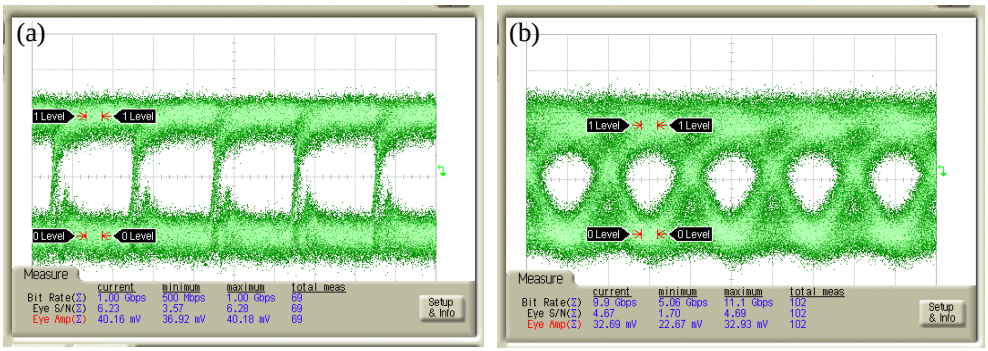

Fig. 10. Eye-diagrams of the optical bus waveguide measured at (a) 1Gbps and (b) 10Gbps.

6. Summary

In summary, we have designed and fabricated 3 × 3 bi-directional optical bus waveguides with embedded 45° micro-mirrors for broadcasting optical signals using metallic UV imprinting method. The high quality nickel mold used in the imprinting processes is fabricated by electroplating metal into pre-defined SU-8 patterns. The optical insertion loss of the bus waveguide is around −15dB due to the complicate structures including bending and splitting waveguides. With the unique broadcasting capability, the implemented optical bus structure successfully demonstrated high speed communication at 10Gbit/sec among multiple points as a high performance optical backplane.

Acknowledgments

This work is supported by the National Science Foundation. The fabrication and characterization facilities at MRC of the University of Texas are supported through NNIN program.

#147768 - $15.00 USD Received 18 May 2011; revised 28 Jun 2011; accepted 1 Jul 2011; published 12 Jul 2011